Simulation of welding temperature distribution, stress and distortion in GTAW process for T-joint

Mô phỏng nhiệt độ, ứng suất và biến dạng của mối hàn chữ T bằng phương pháp hàn GTAW

Ngo Thi Thao[1], Nguyen Van Toan[1,2], Than Van The[1,*]

[1]*Hung Yen University of Technology and Education*

[2]*Bac Ninh College of Electromechanics and Construction*

**Email: thanthe.ck@gmail.com*

Tel: +84-2213713519; Mobile: 0972957980

Keywords:

ANSYS; GTAW; T-joint; Volumetric heat source.

Abstract

The Gas Tungsten Arc Welding (GTAW) process is widely used for welding T-joints of aluminum alloy plate. This paper presents an application of ANSYS software to simulate and predict T-joints' temperature distribution, stress and distortion. The complication in determining the heat source of fusion welding processes is fully provided and considered in this study. A three-dimensional of T-joint fillet weld was built and simulated by using ANSYS. Different welding conditions are utilized during simulation to evaluate effect of each welding parameter on temperature distributions, stresses and distortions. Results indicate that the temperatures and stresses as well as distortion were increased as welding current and voltage increase, and decreased as welding speed increase. Therefore, the simulation can be applied to find primary optimal welding parameters of GTAW for reducing defects and number of welding experiments.

Từ khóa:

ANSYS; GTAW; liên kết chữ T; nguồn nhiệt thể tích.

Tóm tắt

Phương pháp hàn điện cực không nóng chảy trong môi trường khí bảo vệ (GTAW) được dùng rộng rãi cho liên kết hàn chữ T hợp kim nhôm. Trong bài bài náy trình bày việc ứng dụng phần mềm ANSYS để mô phỏng và dự đoán nhiệt, ứng suất và biến dạng của liên kết hàn chữ T. Sự phức tạp trong quá trình xác định nguồn nhiệt khi hàn đã được đưa ra và xem xét một cách đầy đủ. Mô hình 3D của liên kết hàn chữ T được xây dựng và mô phỏng bằng ANSYS. Quá trình mô phỏng với chế độ hàn khác nhau đã được thực hiện để xác định ảnh hưởng của mỗi thông số hàn tới nhiệt độ, ứng suất và biến dạng. Kết quả chỉ ra rằng nhiệt độ, ứng suất cũng như biến dạng tăng khi tăng cường độ dòng và điện áp hàn, và giảm khi tăng tốc độ hàn. Từ đó, nhận thấy rằng, mô phỏng số có thể áp dụng để tìm ra thông số hàn tối ưu ban đầu cho GTAW để giảm khuyết tật cũng như số lượng thí nghiệm.

Received: 20/7/2018

Received in revised form: 03/9/2018

Accepted: 15/9/2018

1. INTRODUCTION

In fact, Gas Tungsten Arc Welding (GTAW) is a very versatile, all-position welding process that is widely used to join most metals and alloys with high weld quality and good welding shape. Heat generation for welding is generated from an electric arc established between a non-consumable tungsten electric and the workpiece. Concentrated arc energy, narrow heat-affected zone, no slag- no requirement for flux, no sparks or spatter-no transfer of metal across the arc, good for welding thin material, good for welding dissimilar metals together are some advantages of this welding method. GTAW has been significantly investigated in recent time. A review on effects of GTAW process parameters on weld was reported by P. P. Thakur and A. N. Chapgaon [1]. FengguiLu, ShunYao, and YongbingLi [2] used finite element method for modeling weld pool in GTAW with different welding parameters to weldment quality. Aluminum is a difficult metal to weld due to the oxide layer that should be removed from its surface before welding. GTAW process is one of the methods used to weld aluminum because it is easy to apply, inexpensive, and produce high quality joints [3]. A weld joint of AA6061 aluminum alloy showed superior mechanical properties compared with GTAW and GMAW joints was studied by A. K. Lakshminarayanan et al. [4].

In most welding processes, welding residual stress and distortion cannot be avoided and they significantly affect weld quality. The basis of stress and distortion analysis is the temperature field during welding [5]. However, in order to calculate and measure them is not easy. In this study, they are estimated by using a simulation software. Among many software applied for mechanical engineering, ANSYS is mostly used because of its advantages. FE model was used to predict precisely the welding deformation and residual stress in a thick multi pass butt welding [6]. A process simulation with ANSYS CFX was applied in arc welding [7]. An equivalent GTAW heat source was successfully estimated and verified by Francois Pichot et al. [8]. The use of non-linear inverse problem and enthalpy method in GTAW process of aluminum was used to determined heat transfer in Al 6065-T5 plate [9]. Arshad AlamSYED [10] used an analytically determined volumetric heat source for modeling of gas metal arc welding process. Most of these studies ANSYS ADPL was used to simulate and predict desired quantities. While the application of ANSYS WORKBENCH in the simulation of welding process is limited.

In this paper, the authors have calculated the heat source and successful application of ANSYS Workbench model and simulate the temperature field using vary welding conditions, resulting in stress and deformation of T-joint fillet weld after GTAW process. Then, the effect of welding parameters on welding temperature and stress as well as distortion is estimated. The result of this article is the basis for the selection of appropriate welding condition to reduce the stress and weld distortion for improving the weldment quality.

2. FINITE ELEMENT MODEL OF GTAW

The fundamental transient heat transfer for a three-dimensional can be described by [10]

$$\frac{\partial}{\partial x}\left(k\frac{\partial T}{\partial x}\right)+\frac{\partial}{\partial y}\left(k\frac{\partial T}{\partial y}\right)+\frac{\partial}{\partial z}\left(k\frac{\partial T}{\partial z}\right)+\dot{Q}=\rho C_p\frac{\partial T}{\partial t} \tag{1}$$

with boundary condition

$$k_n\frac{\partial T}{\partial x}-q+h\left(T-T_0\right)+\sigma\varepsilon\left(T^4-T_0^4\right)=0 \tag{2}$$

in Eqs. (1-2), ρ, k and C_p are density, thermal conductivity and specific heat of workpiece material, respectively; t and T refer to time variable and temperature. $n, k_n, h, \varepsilon, \sigma$ *and* T_0 stand for normal direction to surface, thermal conductivity, heat transfer coefficient ($h=10W/m^2K$ [10]), emissivity, Stefan-Boltzmann constant, and the ambient temperature, respectively. The heat source $\dot{Q}$ can be determined as

$$\dot{Q} = \frac{6\sqrt{3} f_i p\eta}{\pi\sqrt{\pi} a_i bc} \exp\left(-\frac{3x^2}{a_i^2} - \frac{3y^2}{b^2} - \frac{3z^2}{c^2} \right) \tag{3}$$

in which P is the arc power, I and U are the arc current and voltage, $\eta = 0.8$ is process efficiency. The subscript i indicates 1 and 2 corresponding to the front and rear heat source.

Nowadays, ANSYS is become a popular FE software which is applied to model multiphysics phenomenon. In this study, the software is built and utilized for analyzing temperature, stress and distortion in GTAW process of T-joint. Aluminum alloy 6061 with Tensile σ_k and Yield strength σ_c are 124~310 N/mm^2 and 207 N/mm^2, respectively. In addition, the chemical compose is shown in Table 1.

Table 1. Chemical compose of Aluminum alloy 6061 (%)

Name	**Si**	**Fe (max)**	**Cu**	**Mn**	**Mg**	**Zn**	**Ti**	**Other**	**Al**
Al 6061	0.4-0.8	0.7	0.15-0.4	0.15	0.8-1.2	0.25	0.15	0.05	95.8÷98.6

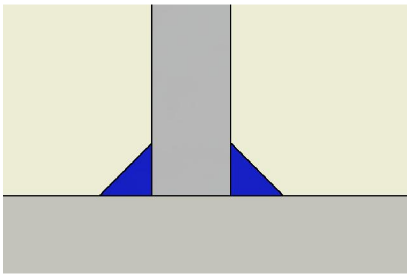

Fig. 1. T-joint model

Fig. 1 depicts the T-joint model with horizontal plate (170 x 210 x 5 mm) and vertical plate (100x210 x 5 mm). Several welding condition (refer to Table 2) is investigated to find welding temperature, stress and distortion.

Table 2. Welding conditions

Welding conditions	**Welding current (A)**	**Welding voltage (V)**	**Welding speed (mm/s)**	**Heat input (J/mm)**
1	160	16.4	4.2	624.76
2	155	16.4	4.2	605.24
3	170	16.4	4.2	663.81
4	160	16.4	3.8	690.53
5	160	16.4	4.6	570.43
6	160	15.5	4.2	590.48
7	160	17.3	4.2	659.05

Whole calculation and simulation of the welding can be summarized as in Fig. 2. All parameters of the welding process is then transfer to the ANSYS for simulating process which includes steps of Preprocessor, Solution and Postprocessor as shown in Fig. 3.

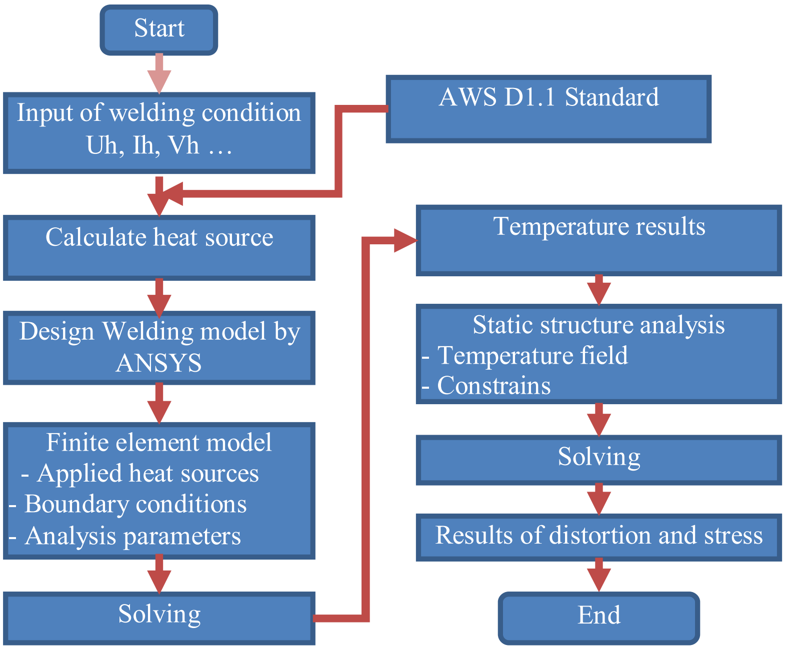

Fig. 2. Flowchart of calculation and simulation processes

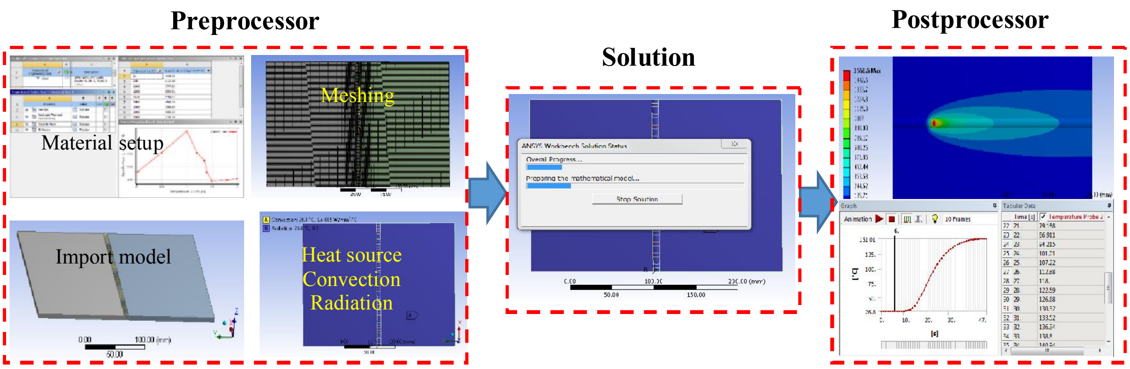

Fig. 3. Simulation procedure

3. RESULTS AND DISCUSSION

Heat generation at condition 1 (U = 16.4 volt, I = 160A, v = 4.2 mm/s) was calculated through Eq. (3) with below variables:

$$r_f = 0.6; r_b = 1.4, [11]$$

$$Q = UI = 16.4 \times 160 \times 0.8 = 2099.2 \ (J/s)$$

$$c_f = r_f R = 0.6 \times 7.76 = 4.66 \ (mm) \text{ and } c_b = r_b R = 1.4 \times 7.76 = 10.86 \ (mm)$$

$$b=\sqrt{R^2-(R-c_f)^2}=\sqrt{7.76^2-(7.76-4.66)^2}=7.11\text{ (mm)}$$

$$a=(2R^3)/[(c_f+c_b)b]=(2\times 7.76^3)/[(4.66+10.86)\times 7.11]=8.47(mm)$$

with x=5.66 mm, y = 2.83 mm, ξ = 4.2 mm

$$V_f=\frac{1}{2}\times 4^2\times 4.2\times 0,3=10.08(mm^3)\text{ and }V_b=\frac{1}{2}\times 4^2\times 4.2\times 0.7=23.52(mm3)$$

$$\dot{Q}=\dot{Q}_f+\dot{Q}_b=\frac{6\sqrt{3}r_fQ}{abc_f\pi\sqrt{\pi}}exp\left(-\frac{3x^2}{a^2}-\frac{3y^2}{b^2}-\frac{3\xi^2}{c_f^{\,2}}\right)V_f+\frac{6\sqrt{3}r_bQ}{abc_b\pi\sqrt{\pi}}exp\left(-\frac{3x^2}{a^2}-\frac{3y^2}{b^2}-\frac{3\xi^2}{c_b^{\,2}}\right)V_b$$

$$=\frac{6\sqrt{3}\times 0.6\times 2099.2}{8.47\times 7.11\times 4.66\times\pi\sqrt{\pi}}exp\left(-\frac{3\times 5.66^2}{8.47^2}-\frac{3\times 2.83^2}{7.11^2}-\frac{3\times 4.2^2}{4.66^2}\right)\times 10.08$$

$$+\frac{6\sqrt{3}\times 1.4\times 2099.2}{8.47\times 7.11\times 10.86\times\pi\sqrt{\pi}}exp\left(-\frac{3\times 5.66^2}{8.47^2}-\frac{3\times 2.83^2}{7.11^2}-\frac{3\times 4.2^2}{10.86^2}\right)\times 23.52=21.73(W/mm^3)$$

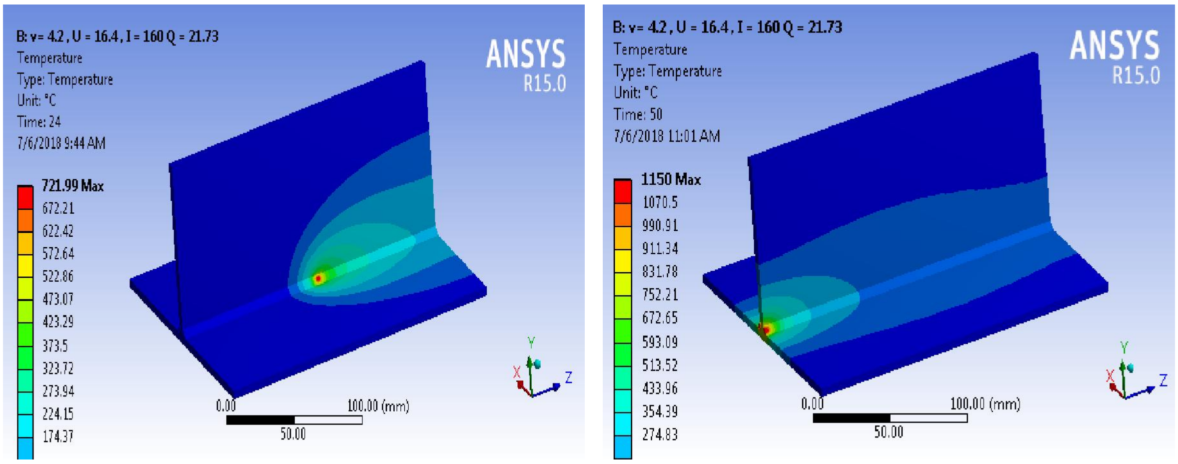

a. Temperature

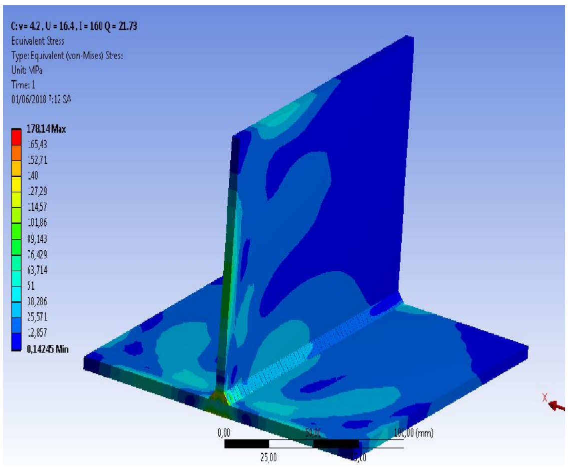

b. Stress

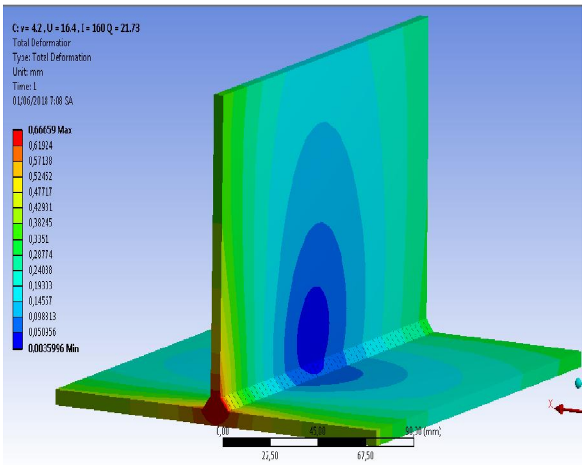

c. Distortion

Fig. 4. Simulation results for welding condition 1

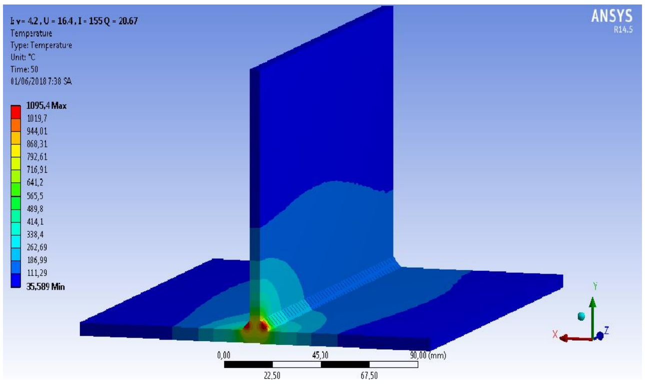

a. Temperature

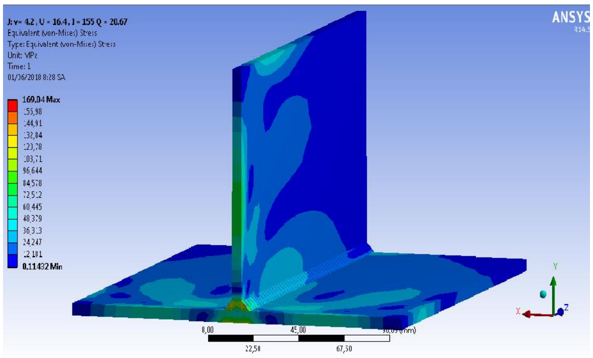

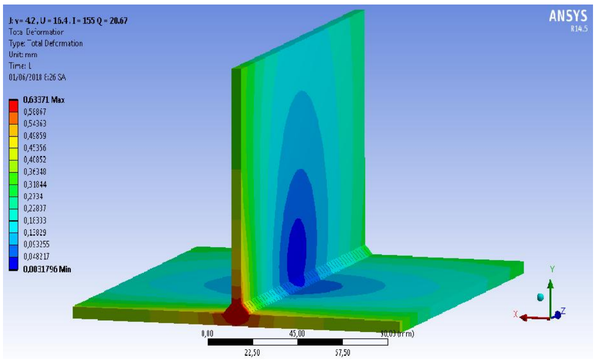

b. Stress c. Distortion

Fig. 5. Simulation results for welding condition 2

Simulation results of welding condition 1 are obtained and presented in Fig. 4. The stable and highest welding temperature are 722^{0}C and 1150^{0}C, respectively. The equivalent stress and the total deformation are subsequently shown in Figs. 4(b) and (c). The maximum equivalent stress and total deformation are 178.14 Mpa and 0.666 mm, respectively.

Fig. 5 indicate the temperature, stress and distortion using welding condition 2. Under decreased welding current at welding condition 2, all results in temperature, stress and distortion are slower than that at welding condition 1. This is because smaller welding current the heat generation input workpieces will be decreased.

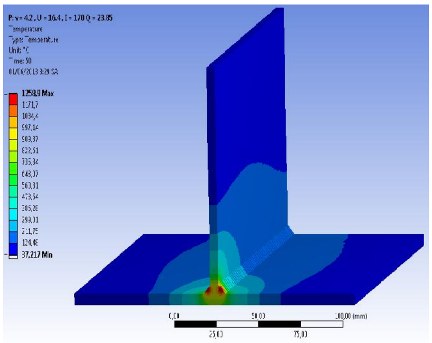

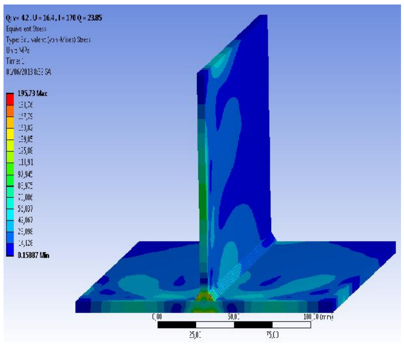

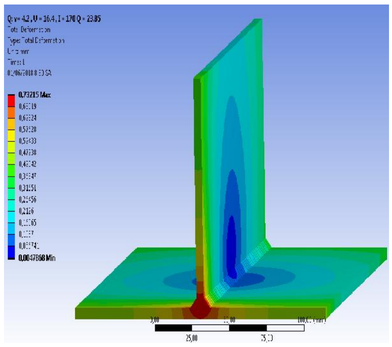

a. Temperature b. Stress c. Distortion

Fig. 6. Simulation results for welding condition 3

Similarly, the maximum values in welding temperature, stress and distribution under welding condition 3 are shows in Fig. 6 at 1258.9 ^{0}C, 195.73Mpa and 0.732mm, respectively. As observed, the higher results were found in Fig. 6 because of higher welding current at condition 3 leading to obtain higher heat flux.

A comparison of the simulation results under different welding conditions are listed in Table 3. Through these results, the effect of welding current on heat generation, welding temperature, stress and deformation are evaluated. It can be seen that all values will increase with increasing the welding current.

Table 3. Simulation results under different welding currents

Results	**Welding condition 2** $I_h = 155(A)$	**Welding condition 1** $I_h = 160(A)$	**Welding condition 3** $I_h = 170(A)$
Heat generation (W/mm^3)	20.67	21.73	23.85
Maximum temperature (^0C)	1095.4	1150	1258.9
Total stress (MPa)	169.04	178.14	195.73
Total deformation (mm)	0.634	0.667	0.732

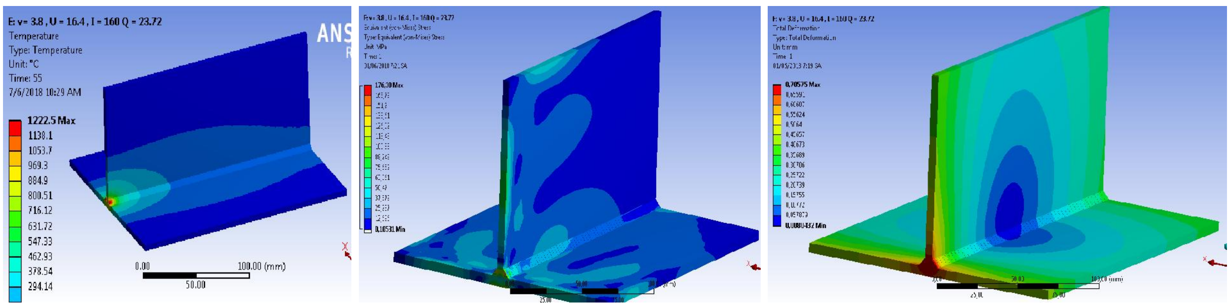

a. Temperature b. Stress c. Distortion

Figure 7. Simulation results for welding condition 4

Moreover, with welding condition of U = 16.4 volt, I = 160A, v = 3.8 mm/s named welding condition 4 (refer to Table 3), the numerical results of temperature, stress and distortion are given in Fig. 7. Temperature results exhibit that with stable arc welding, the maximum temperature is around 745^{0}C at center of welding pool. However, temperature at end of welded process can reach 1223^{0}C. Different temperature zones and isothermal contour are also indicated in the temperature field. From Fig. 7(b), it can be seen that the equivalent stress reaches maximum magnitude at end of welding (176.38Mpa). The total deformation has maximum value of 0.705mm as in Fig. 7(c). The results reveal that the temperature stress and deformation are symmetric.

Table 4. Simulation results under different welding speeds

Results	**Welding condition 4** $V_h = 3.8mm/s$	**Welding condition 1** $V_h = 4.2mm/s$	**Welding condition 5** $V_h = 4.6mm/s$
Heat generation (W/mm^3)	23.72	21.73	19.76
Stable temperature (^{0}C)	745	722	684
Maximum temperature (^{0}C)	1223	1150	1069
Equivalent stress (MPa)	176.38	178.14	183.23
Total deformation (mm)	0.706	0.667	0.619

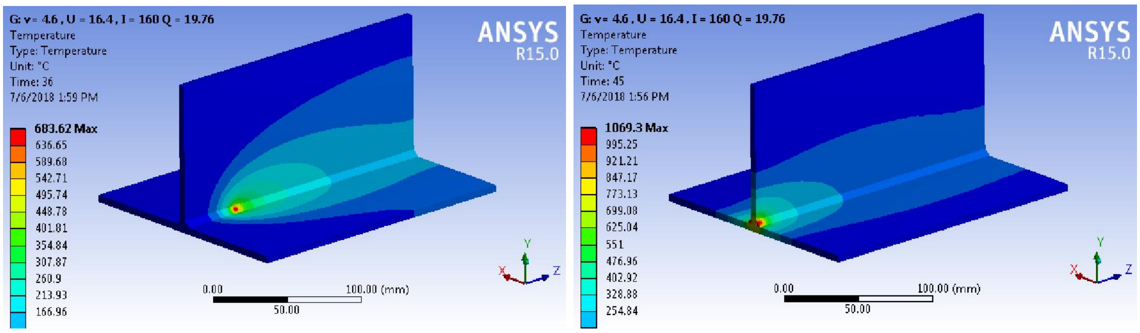

a. Temperature

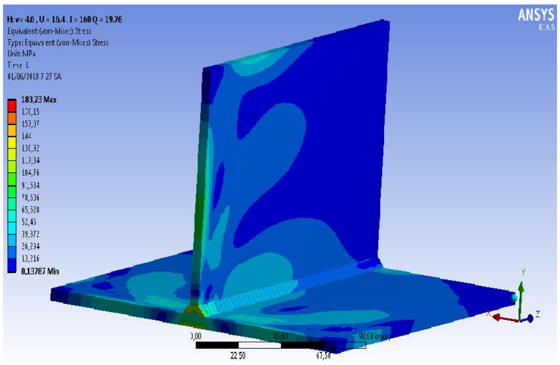

b. Stress

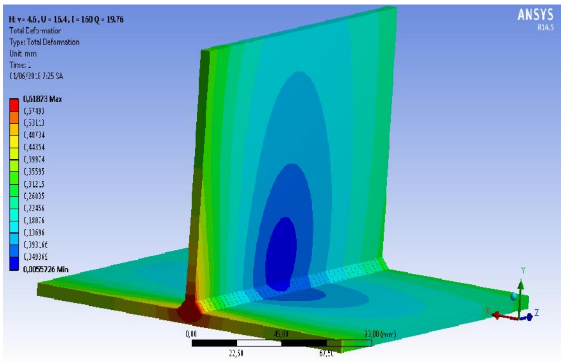

c. Deformation

Fig. 8. Simulation results for welding condition 5

The welding speed has been continuously increased to 4.6 mm/s (welding condition 5). Fig. 8 displays the simulation temperature, stress and deformation. Again, the temperature also is decreased due to increasing welding speed. A comparison of temperature is presented in Table 4. Values of heat generation, stable temperature, maximum temperature, equivalent stress and total deformation are compared together under different welding speeds as given in Table 4. As seen in Table 4, all obtained results were decreased with increase in welding velocity. It may be explained that faster welding speed will provide smaller heat generation generated into welding zone.

Table 5. Simulation results under different welding voltages

Results	**Welding condition 6** $U_h = 15.5(V)$	**Welding condition 1** $U_h = 16.4(V)$	**Welding condition 7** $U_h = 17.3(V)$
Heat generation $\left(W/mm^3\right)$	19.86	21.73	23.59
Maximum temperature (^{0}C)	1053.7	1150	1245.6
Equivalent stress (MPa)	162.11	178.14	193.59
Total deformation (mm)	0.609	0.667	0.724

Finally, welding conditions 6 and 7 were accomplished with different welding voltages (refer to Table 3). As increasing the welding voltage, the heat generation, welding temperature, stress and deformation will be raised as acquired in Table 5. From simulated results, the effect of welding parameters such as welding current, speed and voltage on thermal quantity and stress as well as deformation are fully estimated.

4. CONCLUSIONS

ANSYS software is applied to simulate welding temperature, stress and deformation of aluminum alloy T-joint fillet weld for GTAW process. Different welding conditions were used for simulation to evaluate the effect of welding parameter i.e. welding current, welding speed and welding voltage on welding temperature distribution, stress and distortion. As a result, heat transfer into the workpieces will be varied when changing welding parameters. Obtained results show that the welding temperature, stress and distortion were increased with increasing welding current and welding voltage and decreasing welding speed. The results are the basis for choosing appropriate welding condition to achieve desired temperature and reduce the stress and weld distortion for improving the weldment quality.

ACKNOWLEDGEMENT

This research was supported by Center for Research and Applications in Science and Technology, Hung Yen University of Technology and Education, under the grant number UTEHY.T031.P1819.01.

REFERENCES

[1]. P. P. Thakur , A. N. Chapgaon - International Journal for Research in Applied Science & Engineering Technology (IJRASET),Volume 4 Issue I, January 2016 - A Review on Effects of GTAW Process Parameters on weld

[2]. FengguiLu, ShunYao,SongnianLou,YongbingLi - Modeling and finite element analysis on GTAW arc and weld pool

[3]. Minerva Dorta-Almenara and María Cristina Capace, Microstructure and mechanical properties of GTAW welded joints of AA6105 aluminum alloy, Revista Facultad de Ingeniería (Rev. Fac. Ing.) Vol. 25 (43), pp. 7-19, 2016

[4]. A. K. LakshminarayananV. Balasubramanian, K. Elangovan, Effect of welding processes on tensile properties of AA6061 aluminium alloy joints, The International Journal of Advanced Manufacturing Technology, Volume 40, pp 286–296, 2009.

[5]. Dieter Radaj, Heat Effects of Welding, Springer-Verlag Berlin Heidelberg, 1992, pp 129-246.

[6]. Chand, Reenal R. and Kim, I. and Lee, J. and Jung, S. and Lee, J. (2012) Numerical studies on residual stress and strain distribution in Thick-Welded Plate. Asian International Journal of Science and Technology in Production and Manufacturing Engineering, 5 (4). pp. 65-71. ISSN 1906-151X

[7]. Andreas Spille-Kohoff, Dr. -Arc Welding: From Process Simulation to Structural Mechanics Part I Process Simulation with ANSYS CFX

[8]. Francois Pichot, Michel Danisa, Eric Lacoste, Yann Danis, Numerical definition of an equivalent GTAW heat source, Journal of Materials Processing Technology, Vol 213, 2013, pp 1241- 1248

[9]. E.S. Magalhães, et al. The use of non-linear inverse problem and enthalpy method in GTAW process of aluminum, International Communications in Heat and Mass Transfer, Vol. 66, 2015, pp 114-121

[10]. Arshad Alam SYED, Andreas PITTNER, Michael RETHMEIER, Amitava DE, Modeling of Gas Metal Arc Welding Process Using an Analytically Determined Volumetric Heat Source, ISIJ International, Vol. 53, 2013, pp. 698–703

[11]. Víctor García-García, Juan Cristóbal Camacho-Arriaga, Francisco Reyes-Calderón - A simplified elliptic paraboloid heat source model for autogenous GTA